Photocatalytic degradation of Perchloroethylene by a lab-scale continuous-flow annular photoreactor packed with glass beads carbon-doped TiO$_2$ nanoparticles

Hojjat Kazemi [a,*], Mahboubeh Rabbani [b], Haniye Kashafroodi [b] and Hossin kazemi [a]

[a]Analytical Chemistry Research Group, Research Institute of Petroleum Industry (RIPI), Tehran, Iran
[b]Department of Chemistry, Iran University of Science and Technology, Narmak, Tehran, Iran

ABSTRACT

In this study, the amount of photocatalytic degradation of perchloroethylene in the gas phase was investigated by a fixed bed continuous-flow tubular photoreactor. The photoreactor consists of a cylindrical glass tube, was filled with glass beads coated with nanoparticles of TiO$_2$, and TiO$_2$ doped carbon (TiO$_2$-C). These nanoparticles were synthesized by the sol-gel method and deposited on glass beads using the sol-gel dip technique. X-ray diffraction (XRD), scanning electron microscopy (SEM), Fourier transforms infrared spectroscopy (FT-IR), and diffuse reflectance spectroscopy (DRS) were used for the characterization of synthesized materials. The effect of different parameters such as relative humidity, residence time, PCE concentration on the photocatalytic degradation process was investigated by ultraviolet irradiation to achieve the highest possible degradation efficiency. The PCE degradation and byproduct species were monitored and identified with a gas chromatography-mass spectrometer device (GC-MS). Under the optimum experimental conditions, the photocatalytic activities of TiO$_2$, TiO$_2$-C were investigated and compared together. The results showed that photocatalytic activity of TiO$_2$ for degradation of PCE was extremely increased when doped with carbon. For TiO$_2$-C catalyst, under UV irradiation (3000 ppm initial PCE concentration, 30% humidity and 1 min residence time) approximately 96% of the initial PCE was degraded. Also, the catalyst showed high stability over 48 h without a decrease in catalytically efficiency. All results show that TiO$_2$-C is a good candidate for application PCE degradation.

1. Introduction

Among volatile organic compounds (VOCs) chlorinated volatile organic compounds, such as perchloroethylene (PCE), are important because of widely used as solvents at industrial scale in metal parts, semiconductors washing, dry cleaning, etc.

This extensive use leads to their being extremely present in the water and air. These compounds are toxic, carcinogenic and have many other adverse effects on humans [1, 2]. Therefore, there are great efforts to develop inexpensive and effective processes that can completely degrade these compounds. In the physical methods, the pollutants are only transferred from one phase to another without any degradation. The chemical

methods are expensive, require high doses of chemicals, and produce large amounts of sludge [3]. In recent years, advanced oxidation processes (AOPs) have been used for the degradation and mineralization of the potentially toxic organic and inorganic contaminants in industrial wastewaters [4, 5]. Some AOPs are the photo-catalytic [6], Fenton and photo-Fenton [7, 8], UV/H_2O_2 [9] processes. Heterogeneous photocatalytic oxidation (PCO) appears to be a promising process for eliminating VOCs from the air because of operation at ambient temperature and ability to complete degradation/mineralization of VOCs (by-products are generally harmless CO_2, H_2O and mineral acids) [10, 11]. Many reports described the degradation of PCE through PCO [11, 12]. In these reports, TiO_2 is the most widely used as a photocatalyst because of its high photocatalytic activity, non-toxicity, and stability [13, 14]. Although TiO_2 itself has been proved to be a suitable photocatalyst for oxidation of PCE through PCO, more efforts are needed for further improvement of photocatalytic performance of TiO_2-based catalysts. Supporting on materials with large surface areas such as glass fiber [15], paint [16], thin-film TiO_2 [17], TiO_2 pellet [18], carbon black or activated carbon [19], carbon nanofibers [20], carbon nanotube [21] is one approach. Another trend is combining or doping TiO_2 with other materials such as Ag [22], Au [23], Sn [24], Pb [25], Ni [26] metal oxides [27] to improve the performance of the photocatalyst. Among these attempts, TiO_2 doping with transition metals ions such as V, Co, or Fe has been a common approach for improving the photocatalytic performance of the catalyst. However, some key problems remain unresolved, for example, doped materials suffer from thermal instability, photo-corrosion, and an increase in the carrier-recombination probability. Non-metal (B, F, N, C etc.) doping has since proved to be far more successful. Especially, in the process of carbon doping, the C element is always suggested permeating to the lattice of TiO_2 substituting a lattice O atom and forming O–Ti–C species [28-31]. Another approach is to change or

design new reactor configurations. Some reactor configurations are honeycomb monolith, plate, fluidized bed, packed bed, and annular tube flow [32, 33]. The design of the photocatalytic reactor plays an important role in its photocatalytic performance. Some factors such as specific surface area, pass-through channels, air velocity, direction and angle of irradiance of UV light on the catalyst surface, contact area and a mass transfer should be considered in the design of a photocatalytic reactor [32, 33].

In this project, a fixed substrate filled photocatalytic system was used, with a light source in its center, which in other words, is a combination of a filled and ring-shaped system. On one hand, the advantage of ring-shaped tube systems was used for direct light radiation to the reaction surface taking into account placing the light source in the center of the system, which reduces the number of bulbs as well as the effective use of diffused light from an optical source in different directions and, on the other hand, a greater contact surface between the catalyst and the pollutant in the fixed substrate system was created. The rotating center system is designed for two rows of glass balls to be placed nearby each other, this design increases the contact surface of the pollutant with the catalyst compared to other systems. Also, direct light radiation to glass balls can cause light fractions in any ball and increase light intensity throughout the system. In general, the system is designed to utilize all the power and efficiency of the catalysts by increasing the reaction surface and the immediate light exposure. That's why in this work, we report an experimental study of the photocatalytic oxidation of PCE in the gas phase using a lab-scale continuous-flow annular photoreactor packed with glass beads. TiO_2, C doped TiO_2 nanoparticles synthesized with the sol-gel method and deposited at the surface of glass beads with dip-coating technique. The performance of the photoreactor was evaluated for different operating conditions, such as feed flow rate, PCE concentration, residence time and relative humidity. To prove efficiency in industrial

applications, the effect of these parameters was investigated under the same industrial condition. For this propose, High concentrations of PCE (between 574 and 2442 ppm), a large range of air stream flow rates contaminated with PCE (59–300 mL min^{-1}, measured at 298 K and 1 bar) and different water vapour contents (12–40%, measured at 298 K and 1 bar) were employed.

2. Experimental
2.1. Materials
All the solvents and chemicals were purchased from Merck and Sigma-Aldrich Companies and used without further purification. The glass beads with a diameter of 5-6 mm were used as a support material and deionized (DI) water was used to prepare the different solutions and washing steps.

2.2. Instruments
The X-ray diffraction (XRD) patterns were recorded by a Philips Xpert X-ray diffractometer (Model PW1729) with Cu Kα radiation. The Structures and morphologies of nanoparticles were determined using scanning electron microscopy (SEM, TE-SCAN model MIRA3). The Fourier transform-infrared (FT-IR) spectra were obtained using BRUKER spectra VERTEX apparatus. The UV-VIS diffuse reflectance spectra (DRS) were recorded by a DRS apparatus (Shimadzu UV-1800). The identification of photodegradation by-products was done by a gas chromatography-mass spectrometry (GC-MS) system (Shimadzu, QP-2010SE).

2.3. GC/MS analysis
The identification of product gas streams and intermediate products were analyzed employing a gas chromatography-mass spectrometry (GC/MS) system operating in electron impact mode using an HP-5 (30m × 0.25mm × 250μm) capillary column. The GC column was operated in a temperature-programmed mode with an initial temperature of 35° C held for 5 min, ramp at 4° C min^{-1} up to 250° C and held at that temperature for 5 min. Injector temperature was 280° C with helium serving as

the carrier gas at the flow rate of 2 mLmin^{-1}. The identification of photodegradation products was done by comparing the GC/MS spectra patterns with those of standard mass spectra in the National Institute of Standards and Technology (NIST) library.

2.4. Catalyst base preparation method
Before the synthesis, transparent glass beads (with a diameter of 5-6 mm) were roughened mechanically by sandblasting method to increase surface area and adherence between the catalyst and the support. The surface glass beads were physically roughened in a mixture of water, sandblasting sand and sanding powder using a mechanical mixer and then etched in 1M NaOH solution. After sandblasting, the glass beads were washed sequentially and thoroughly with acetone, ethanol and deionized water (DW). Then they were dried at 80 °C for 1 h in the oven [34].

2.5. Synthesis of TiO$_2$, C doped TiO$_2$ supported on roughened glass bead
TiO$_2$, C doped TiO$_2$ were prepared via sol-gel method according to the previous reports [34] with few modifications. Briefly, for preparation of carbon-doped TiO$_2$ 50 mmol of Tetrabutyl Orthotitanate (TBOT) was slowly added to a solution of ethanol and water under continuous magnetic agitation at room temperature. Then 4 ml of Hydrochloric acid 1M was added. The resulting mixture was kept stirred for 3 hours at a speed of 500 rpm and then the roughened glass beads were added to the liquid mixture. After 10 minutes, glass beads were separated and dried at 80 ° C for 1 hour and calcinated at 200 ° C for 5 hours, using a heating rate of 1° C min^{-1}. Pure TiO$_2$ was also synthesized with the same procedures as described above, except calcination temperature for the synthesis of pure TiO$_2$ was set at 350° C.

2.6. Photocatalytic reactor
In this study, Photocatalytic degradation of PCE in the air using titanium oxide base (TiO$_2$, TiO$_2$-C) catalysts was evaluated in a lab-scale continuous-

flow tubular UV-photoreactor packed with coated glass beads. The continuous gas flow photoreactor with the length of 40 cm has consisted of two coaxial tubes. The coated glass beads filled the void in-between two coaxial tubes and the inner tube was made of quartz glass housing the light source. The outer tube was a Pyrex tube packed with catalyst coated glass beads to a height of 27 cm which provided an effective volume of 200 ml in the reactor. The external wall of the cylinder was completely covered with a layer of aluminum sheet, so that the light is constantly reflected inside the cylinder. The light source was an 8-watt fluorescent lamp (Philips UVC 8W T5) to provide light with appropriate energy in the ultraviolet region. The reactor feed was prepared by mixing of PCE vapors, humid and dry air which were generated via passing the air through two glass impingers containing pure liquid PCE and distilled water. PCE concentration and humidity were adjusted by controlling flow rate of dry air into the impingers and the amount of dry air entering the mixing tank. The concentration of PCE in the inlet and outlet streams of the photoreactor and degradation byproduct were measured by a GC/MS. humidity and CO_2 content were measured by a SAMWON ENG SU-503B device and a KIMO AQ-100 CO_2 meter, respectively and rechecked by titration methods (Fig.1). All flow rate of was adjusted by a rotameter and the degradation efficiency was measured by equation 1:

$$\text{Degradation Efficiency} = \frac{C_{inlet} - C_{outlet}}{C_{total}} \times 100$$

(Eq.1)

C_{inlet}, C_{outlet} and C_{total} were concentrations of inlet and outlet and total of PCE respectively.
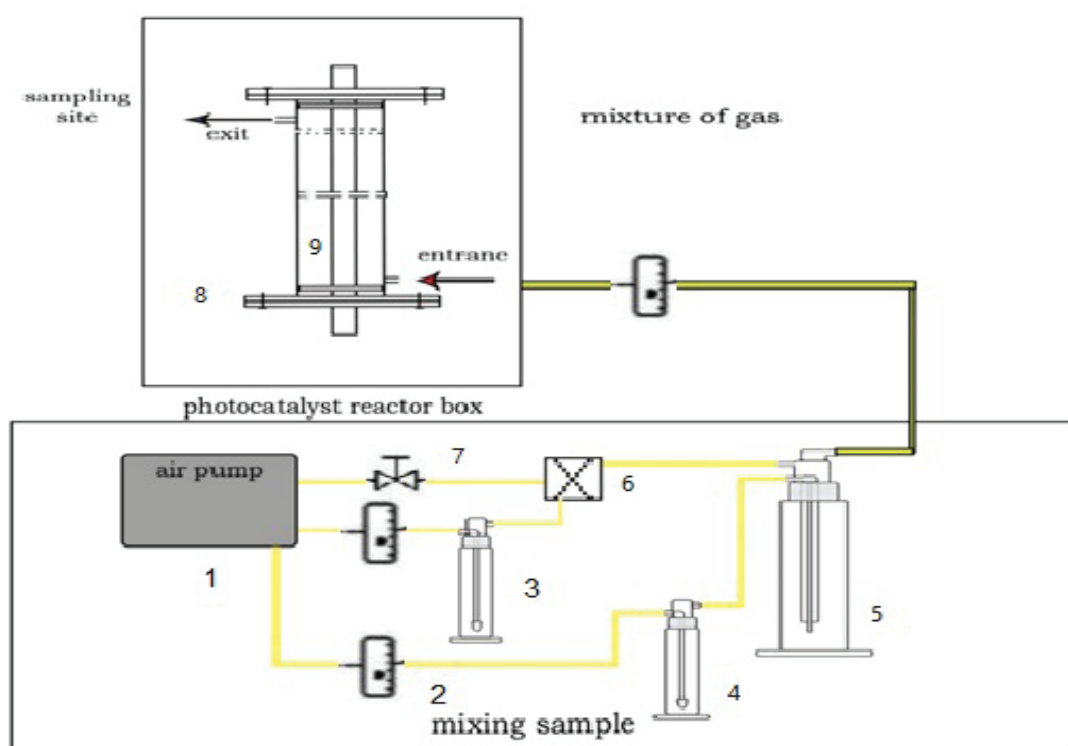

Fig.1. Schematic of photocatalytic system 1) Air reservoir 2) Rotamer 3) Impinger containing water 4) impinger containing Perchloroethylene 5) Mixing chamber 6) Tee 7) Tap 8) Reactor 9) Light source

3. Results and discussion

3.1. Photocatalyst characterization

The synthesized materials were first characterized with X-ray diffraction as shown in Figure 2. Fig. 2 shows a typical XRD pattern of the pure TiO_2 and TiO_2-C which is in good agreement with the standard patterns for anatase titanium dioxide (JCPDS 21-1272) [35] and confirm the absence of any other impurity. The XRD pattern of the TiO_2-C was identical to pure TiO_2 but strongest peak at $2\theta = 25.3°$ (representative of (101) plane). Compared with pure TiO_2 shifted slightly to a higher 2θ value. Also for all synthesized materials, diffraction peaks were weakened and broadened, suggesting distortion of the crystal lattice. Greater change can be seen with the addition of carbon and vanadium, indicating that vanadium and carbon were incorporated into the lattice and greater distortion of the crystal lattice was accorded [36, 37].however, this is favorable for photodegradation purposes because of increasing pathways for gas-phase penetration into the inner spaces of the active materials and increasing of material transportation.

The IR spectrum of TiO_2 and TiO_2-C were shown in Figure 3. The FT-IR spectrum of both spectra displays absorption bands between 700 and 800 cm^{-1}, which can be assigned to the metal-oxygen stretching vibrations of Ti-O [38]. The broad peak in the range of 3400 nm and sharp peak in the range of 1620 nm corresponds to the stretching and bending bonds of the water molecule, respectively, which occur due to lack of inter-tissue water or the absorption of moisture on the surface of the synthesized materials. The two peaks appearing in 1350 and 1200 nm of the TiO_2-C compound are related to the CH_3 and CH_2 bending bonds, which confirms the presence of carbon in the structure of this compound [18, 39].
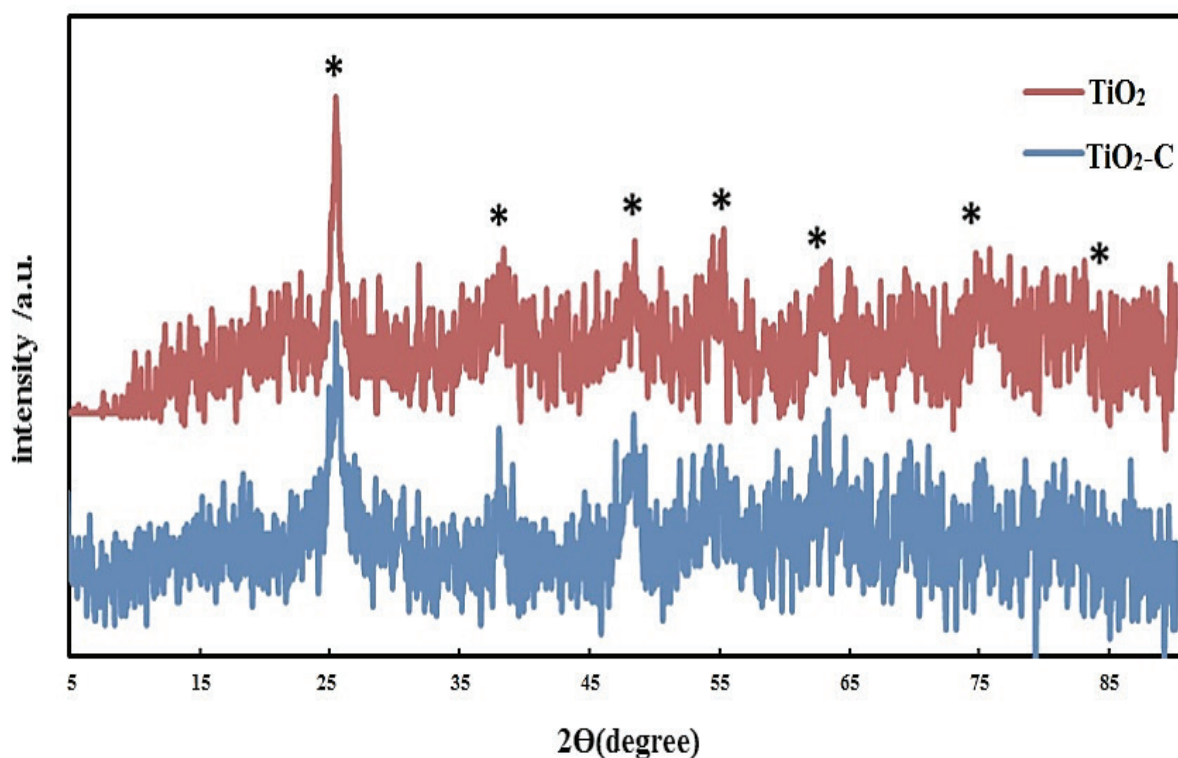

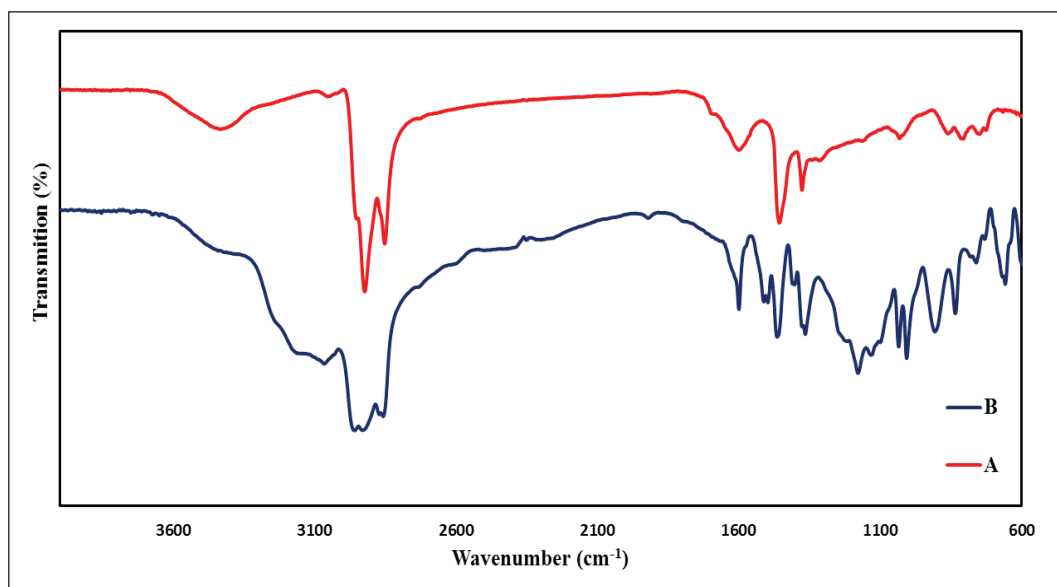**Fig.2.** XRD pattern of the pure TiO_2 and TiO_2-C

Fig.3. FT-IR spectrum of A) TiO_2 and B) TiO_2-C

The optical absorption property is an important factor to influence the photocatalytic activity of the catalysts. Thus, the absorbance properties of as-prepared TiO_2 and TiO_2-C were analyzed by the UV–vis diffuse reflection spectra (DRS), and the results are shown in Figure 4. Pure TiO_2 shows the absorbance in the UV region, in which the absorption start point of TiO_2 is around 400nm. While TiO_2-C exhibits good absorption in the UV region and the broad absorption region with less intense in the visible light. Compared with pure TiO_2, TiO_2-C absorbed photon energy in the visible region up to 700 nm indicating that the incorporated elemental carbon was acting as a photosensitizer [40]. The results suggest that TiO_2 and TiO_2-C photocatalysts have higher photocatalytic performances in the UV region.

The morphology of the fabricated products was characterized by scanning electron microscopy (SEM) and the results are shown in Figure 5. As seen in Figure 5 the synthesized particles have mostly a spherical morphology with the obtained size in the range of about 14-45 nm for TiO_2 and TiO_2-C.
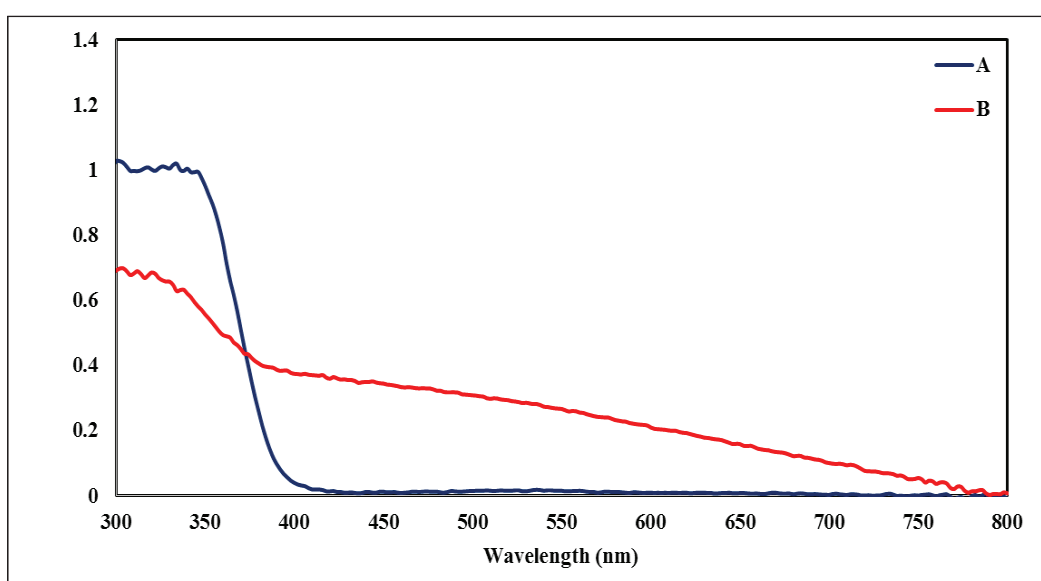

Fig.4. UV–vis diffuse reflection spectra A) TiO_2 and B) TiO_2-C
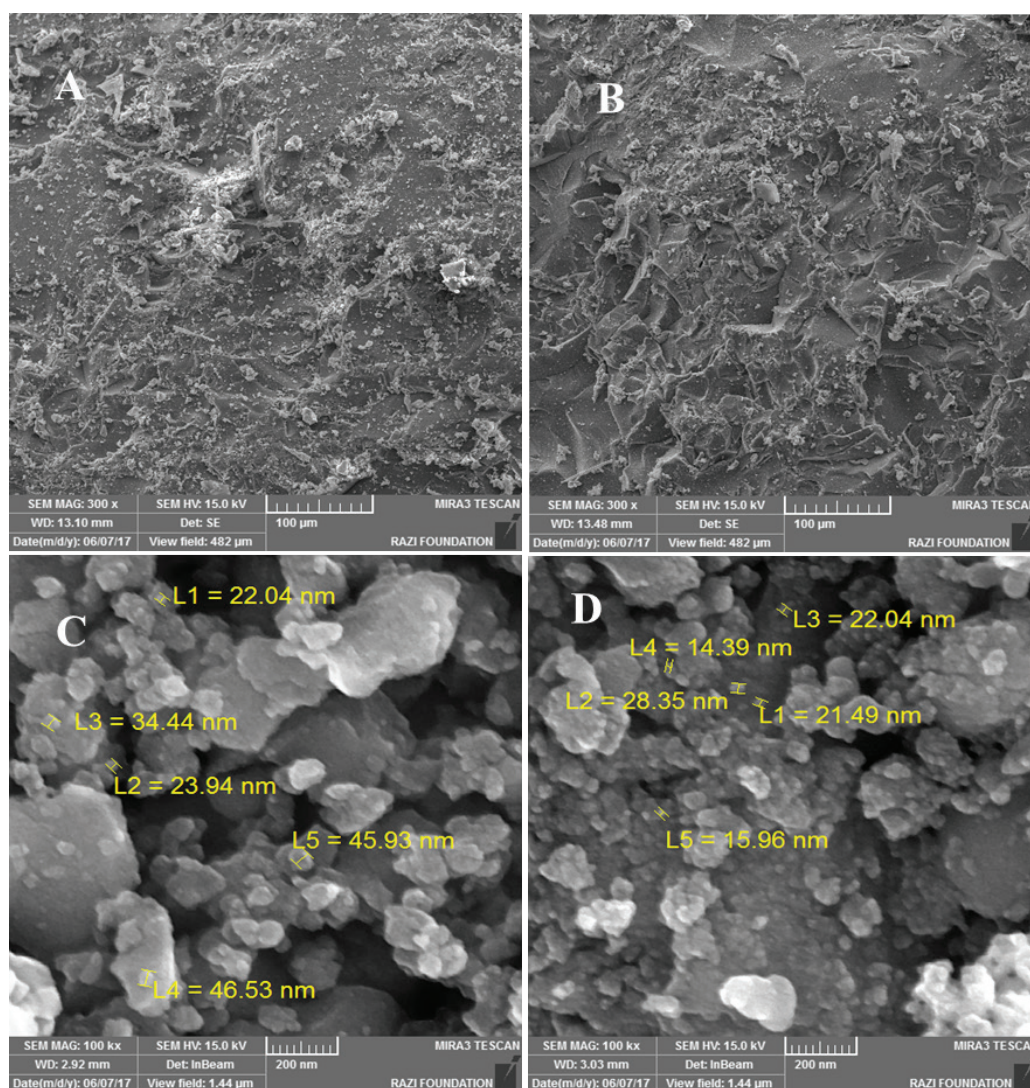
Fig.5. SEM image of (A, C) TiO$_2$ and (B,D) TiO$_2$-C

3.2. Investigating the reaction conditions of photocatalytic system

3.2.1. Concentration effect

First, the degradation efficiency of PCE using TiO$_2$-C photocatalyst in different inlet feed concentrations from 400 to 5000 ppm under UV irradiation, the residence time of 1 min and flow rate 200 mL min^{-1} investigated. Figure 6 is illustrated the effect of increasing PCE feed concentrations on photocatalytic degradation efficiency. As shown, degradation efficiency increased by increasing PCE concentration up to 3000 ppm and rich to 99%, indicating higher PCE means higher adsorption in the surface of the photocatalyst, and higher mass transfer between the PCE gas and the catalyst surface which increased the PCE degradation. Further PCE concentration caused a decrease in the degradation efficiency, because of surface flooding of photocatalyst [41s, this referenceshowed in supporting nformation page, SIP]. It was seen that the degradation capacity of this system is 3000 ppm, which is much higher than that other of reported photocatalytic systems with the same lamp.
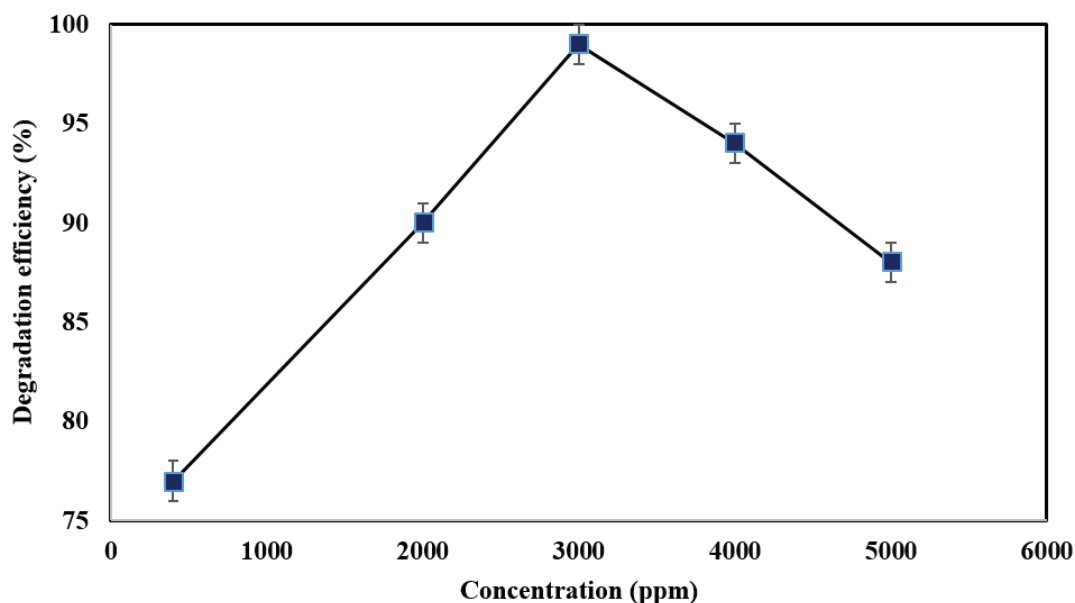
Fig.6. The effect of concentration on degradation efficiency of TiO$_2$-C at a fixed time of 1 min

3.2.2.Residence time effect

Figure 7 shows the residence time effect on degradation efficiency of TiO$_2$-C photocatalyst over the range of the residence times from 0.2 min to 2 min at a 3000 ppm PCE concentration. Residence time in the reactor was controlled by changing the flow rate. As shown for photocatalyst, the PCE degradation increased with increasing residence time, because PCE stays longer inside the reactor and have more opportunity to react with photocatalyst [18]. The increasing residence time of more than 1 min for photocatalyst did not only increase significantly in the degradation efficiency of PCE but also increased the elimination time. As a result, the time of one minute was chosen as the optimal time.
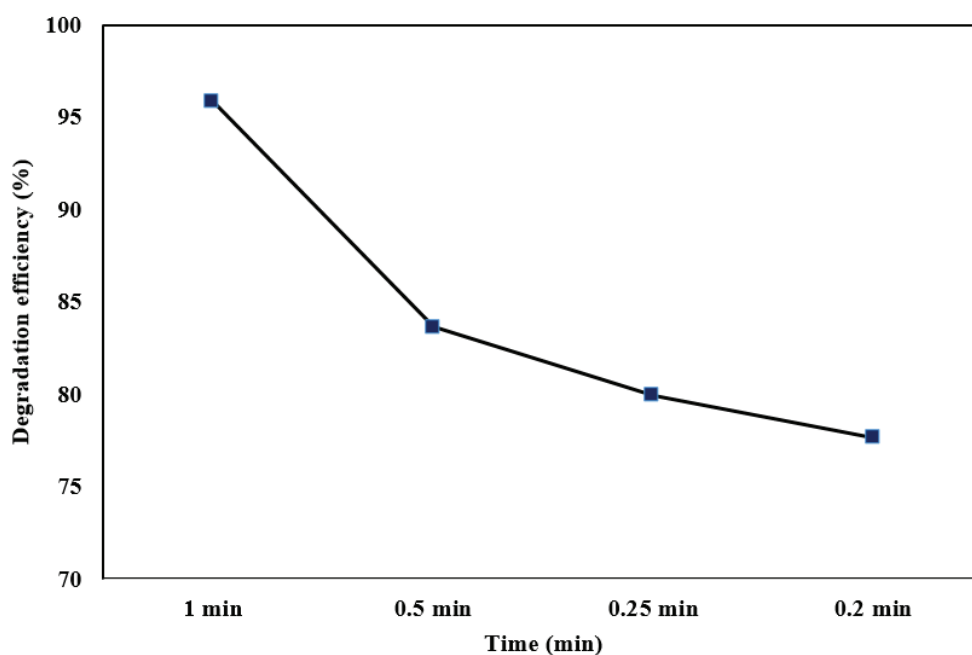

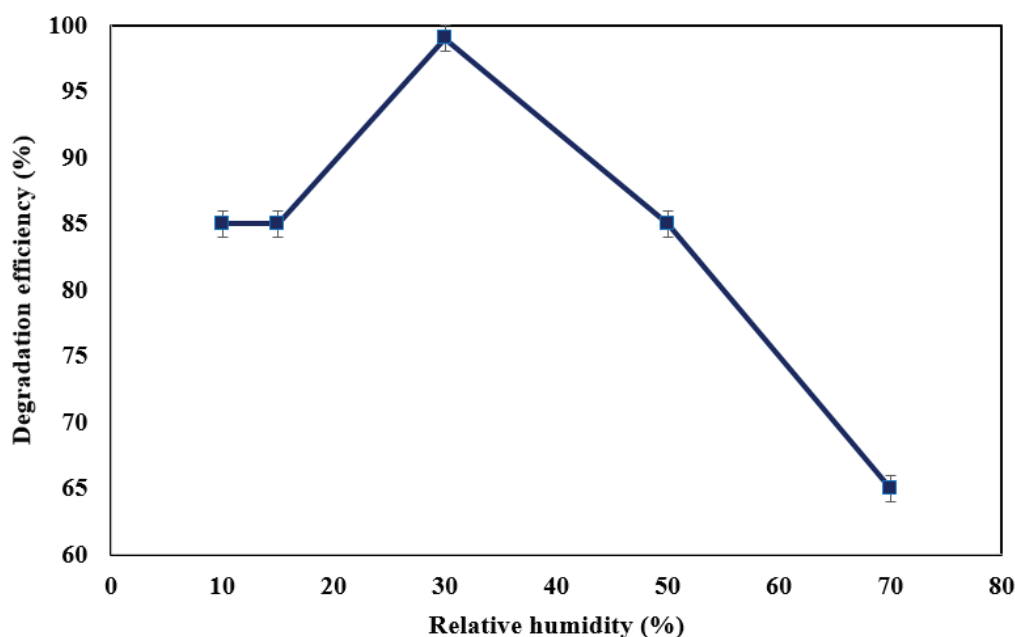**Fig.7.** the effect of time on degradation efficiency of TiO$_2$-C at 3000 ppm

Fig.8. The effect of relative humidity on degradation efficiency of TiO$_2$-C at constant concentration and time of 3000 ppm, 1 min respectively

3.2.3. Moisture Effect

Due to Figure 8, the effect of the water content on the PCE degradation over TiO$_2$-C was evaluated under five relative humidity (RH) conditions (10, 15, 30, 50 and 70%), 3000ppm PCE concentration, one-minute resistance time and UV irradiation. Figure 8 shows that the degradation efficiency of PCE attained under each RH condition. As shown, a significant change in degradation efficiency was not observed as the RH increased from 10 to 15 % but when RH increased up to 30% degradation efficiency increased and rich to approximately 99%. Further increasing of RH reduced the degradation efficiency due to competitive adsorption of PCE and water molecules on the photocatalytic surface. Actually, by more increasing the moisture content of the incoming gas, most photocatalytic active surfaces are coated with water and remaining less surface to contact with PCE and its degradation [14, 42s, SIP]. The opposing effect of the water content has already been discussed in several research works and even so it still is a matter of debate [42s-45s, SIP]. Several authors reported that the absence of water vapour can seriously retard the degradation of several chemicals and their mineralization to CO$_2$ may become incomplete, but excessive water vapor may inhibit the degradation by competitive adsorption on the photocatalyst surface [14].

3.3. Photocatalytic degradation

The photocatalytic performance of prepared samples was evaluated by the PCE degradation under UV light. For comparison, the photocatalytic activity of pure TiO$_2$, TiO$_2$-C $_2$ was also determined under the optimal conditions (eg. 1 min residence time, 30% RH and 3000 ppm PCE concentration). First, the photocatalytic system was filled with glass balls without a photocatalyst coating. Then, the degradation efficiency was studied in the presence of photocatalysts coated glass balls. When the lamp was illuminated, the output of the system was sampled at different times, and the process of changes in concentration, efficiency and output products was investigated by the GC-MS. For the photolysis process (without using any photocatalyst), the system's efficiency was determined 99% based on the reduction of perchloroethylene concentration in

120 min. At first, it seemed that the lamp alone was able to degrade perchloroethylene and perform the complete reaction of converting perchloroethylene to carbon dioxide, water and hydrochloric acid. But after a long time, we observed a large volume of solid crystals at the end of the system and the outlet pipe. By identifying these materials with GC-MS, we realized that most of the material has converted into compounds that result from a simple breakdown of Perchloroethylene bonds. That's why we measured system efficiency based on CO_2 gas. Also, the system's efficiency was calculated 10% based on the produced amount of CO_2 gas. So that the lamp was not capable of completely degrading PCE, merely transforming it into other materials with more complex structures and converting has a small fraction of it into complete degradation reaction products. Also, the system's efficiency was obtained 58% and 95.6% for TiO_2 and TiO_2-C, respectively based on the produced amount of CO_2 gas. The results indicate that in the case of using TiO_2-C, the PCE degradation is almost complete

and turns into completed reaction products in its output, which indicates the correct choice of the pollutant, ie carbon in improving photocatalyst. Table 1 summarizes the major intermediate compounds identified.
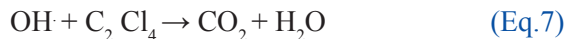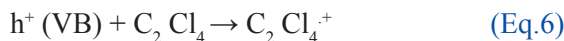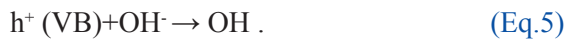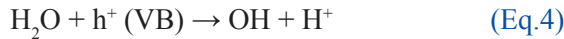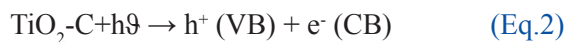
3.4. Photocatalytic mechanism for PCE degradation

For photocatalytic oxidation, an important step of photoreaction is the formation of the hole-elect pairs which need the energy to overcome the band gap between the valence band (VB) and conduction band (CB) [41s,SIP]. TiO_2 as a semiconductor has a valence band and a conduction band. When photocatalyst exposes to UV light, TiO_2 can absorb UV light and electrons transfer from the valence band (VB) to the conduction band (CB) and generate electron-hole pairs (Eq.2) [46s, SIP]. Electrons of CB can react with oxygen adsorbed on the catalyst surface to produce oxygen radicals (O_2^-) (Eq.3). Holes of VB can react with H_2O to produce ·OH radicals (Eq.4, 5). Also, the electrons and the holes

Table.1. Products obtained from photocatalytic degradation of perchloroethylene with UV lamp alone and UV lamp with, TiO_2 and TiO_2-C

Photocatalyst	Compound
UV lamp	H_2O
	C_2Cl_4
	Dichloroacetic acid
	Trichloro dehydrate
	Trichloroacetic acid
UV lamp -TiO_2	H_2O
	HCl
	C_2Cl_4
	Trichloroacetyl chloride
	Methyl trichloroacetate
	Trichloroacetic acid
UV lamp -TiO_2-C	H_2O
	CO_2
	HCl
	C_2Cl_4

may react directly with PCE molecules leading to the formation of oxidizing species (Eq.6) [14, 31, 47s, 48s, SIP]. The radicals (·OH)as a strong oxidizing species and O$_2^{·-}$ are responsible for the degradation of PCE. These ·OH and O$_2^{·-}$ which are produced as shown, further react with C$_2$Cl$_4$ to produce CO$_2$ and water, as represented in (Eq.7, 8) [31, 49s, SIP]. In the absence of suitable electron and hole scavengers, the stored energy is dissipated in a few nanoseconds, through recombination. In some works [50s-52s, SIP], researchers believe that carbon materials can generate photoelectrons and photo holes under UV irradiation. The C element is not directly involved in the photocatalytic process but can absorb UV light. After absorbing enough energy, these regions can generate photoelectrons and photoholes that can be transferred to TiO$_2$. The results obtained show enhancement in the photocatalytic activity when the C element is doped on the surface of TiO$_2$ nanoparticles.

$$TiO_2\text{-}C + h\vartheta \rightarrow h^+ (VB) + e^- (CB) \qquad (Eq.2)$$
$$O_2 + e^- (CB) \rightarrow O_2^- \qquad (Eq.3)$$
$$H_2O + h^+ (VB) \rightarrow OH + H^+ \qquad (Eq.4)$$
$$h^+ (VB) + OH^- \rightarrow OH· \qquad (Eq.5)$$
$$h^+ (VB) + C_2Cl_4 \rightarrow C_2Cl_4^+ \qquad (Eq.6)$$
$$OH· + C_2Cl_4 \rightarrow CO_2 + H_2O \qquad (Eq.7)$$
$$O_2^· + C_2Cl_4 \rightarrow CO_2 + H_2O \qquad (Eq.8)$$

Based on observed products for TiO$_2$-C, several mechanisms of PCE degradation and intermediates have been described in the literature [14, 53s, 54s].

3.5. Photocatalyst stability
The stability of photocatalyst TiO$_2$-C was investigated for a relatively long time to evaluate its capability of being applied in real systems in addition to examining its stability (Fig. 9). Figure 9 shows the change of degradation efficiency over relatively long periods for TiO$_2$-C with 3000 ppm input concentration of PCE, 1min residence time and 30% RH under UV irradiation by the full intensity of the 8W 365 nm lamp. As seen for photocatalysts, first the degradation efficiency was increased and rich to 95% for TiO$_2$-C respectively. No change over 5 hours' periods of time of irradiation were observed. Long term stability was also investigated for TiO$_2$-C photocatalyst over 7 days (result not shown) at the same condition. No change in the stability and degradation efficiency were discernible over this period. These results showed degradation efficiency of TiO$_2$-C was better than TiO$_2$ and relatively50% more than TiO$_2$ and also a good stability over long period of time for TiO$_2$-C, indicating TiO$_2$-C has good efficiency for photocatalytic degradation of PCE and is a good candidate for use in real systems.
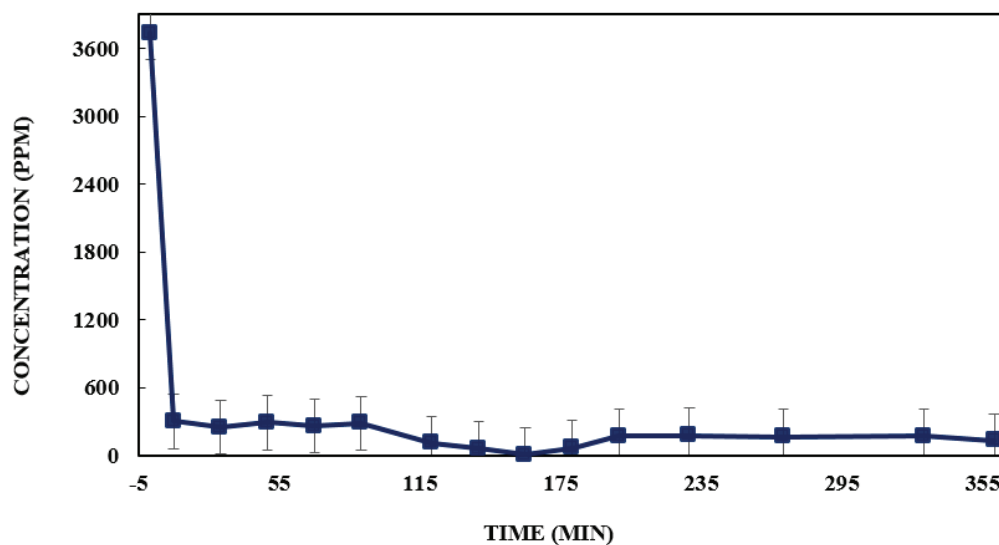

Fig. 9. Photocatalyst stability of TiO$_2$-C over time 5 h

3.6. Comparison of TiO₂-C photocatalyst with other reported works

In Table 2, the different photocatalysts are compared in terms of lamp intensity, degradation wavelength, efficiency, and moisture content. Two factors of lamp power and temperature are very effective in degradation efficiency. On the other hand, in many previous studies, the method of determining the efficiency is expressed merely based on reducing the PCE output and does not consider the conversion of PCE to products and the production of CO_2. In terms of lamp power, the lamp used in the present study has a power of 8 (wat) and a wavelength of 365 nm in the UV region which was one of the least powerful lamps used in this field, indicating the high efficiency of the system due to the design of the lamp. In the center, its large reflection due to the aluminium sheet in the outer wall, the increase in

contact surface due to the use of glass balls and the proper selection of carbon contaminant. Also, the efficiency of the present research, despite the low power consumption (compared to the UV lamps), and the number of fewer lamps, are more or equal than to many previous reports.

4. Conclusions

In this project, a photocatalyst system with a fixed substrate and a light source in its center was used. In general, the system was designed to use all the power and efficiency of the catalysts, by increasing the reaction surface and the direct impact of light. In this system, an 8w fluorescent lamp with a wavelength of 365 nm was used as a source of UV light. The system was filled with glass balls coated with three catalysts (TiO₂, C-TiO₂) synthesized by the sol-gel method and uncoated balls to remove

Table.2. Comparison of TiO₂-C with photocatalysts reported in previous scientific papers

Lamp	Wavelength	Efficiency	Catalyst	Humidity	Reference
A Philips UV A lamp (Cleo performance 80W/10 Model)	The wavelength of 365 nm.	Is not limited	PC500	45 to 55%	[11]
Phillips, 4 W, F4 T5/BLB type	maximum emission at 365 nm	50%	-	-	[1]
three 8W black-light fluorescent lamps	light 365 nm	-	P25Pt/TiO₂ and Pd/TiO₂,	-	[55s]
Philips TL 18W/08 F4T5/BLB	355nm	Predicted conversions show good	Tio₂	48%	[56s]
five black light blue fluorescent lamps (Philips TL 8W/08 F8T5/BLB)	343 and 400	(55%)	(P-25)	8% relative humidity	[57s]
seven(Philips TL 4W/08 F4T5/BLB)	310 to 410 nm	24, 50, and 100%	Tio₂	10, 50, and 90%	[58s]
Eight-4W fluorescent black light bulbs (Toshiba, FL 4BLB)	-	99.3%	Tio₂	-	[59s]
A fluorescent black light bulb (Toshiba, FL 4BLB, 4 W)	-	80%	Porous TiO₂	-	[60s]
1700 W air-cooled Xenon Lamps		Close to 100%	P25 and PC500	20%	[14]
Phillips UVC/8W/T5)	wavelength 365 nm.	99/6%	Tio₂-C	30%	Present study

the pollutants. Among these four samples, the highest and fastest total photocatalytic degradation efficiency was related to the TiO$_2$-C catalyst. The catalyst also had the highest stability and highest degradation efficiency. After degradation, all chemical products were determined by GC-MS analyzer.

5. Acknowledgements

6. References

[1]   K.-S. Lin, N.V. Mdlovu, C.-Y. Chen, C.-L. Chiang, K. Dehvari, Degradation of TCE, PCE, and 1, 2–DCE DNAPLs in contaminated groundwater using polyethylenimine-modified zero-valent iron nanoparticles, J. Clean. Prod., 175 (2018) 456-466. https://doi.org/10.1016/j.jclepro.2017.12.074

[2]   F.V. Lopes, R.A. Monteiro, A.M. Silva, G.V. Silva, J.L. Faria, A.M. Mendes, V.J. Vilar, R.A. Boaventura, Insights into UV-TiO2 photocatalytic degradation of PCE for air decontamination systems, Chem. Eng. j., 204 (2012) 244-257. https://doi.org/10.1016/j.cej.2012.07.079

[3]   A. Gupta, A. Pal, C. Sahoo, Photocatalytic degradation of a mixture of Crystal Violet (Basic Violet 3) and methyl red dye in aqueous suspensions using Ag+ doped TiO$_2$, Dyes and Pigments, 69 (2006) 224-232. https://doi.org/10.1016/j.dyepig.2005.04.001

[4]   A.G. Akerdi, S.H. Bahrami, Application of heterogeneous nano-semiconductors for photocatalytic advanced oxidation of organic compounds: A Review, J. Environ. Chem. Eng., 7 (2019) 103283. https://doi.org/10.1016/j.jece.2019.103283

[5]   A. Fernandes, M. Gągol, P. Makoś, J.A. Khan, G. Boczkaj, Integrated photocatalytic advanced oxidation system (TiO2/UV/O3/H2O2) for degradation of volatile organic compounds, Sep. Purif. Technol., 224 (2019) 1-14. https://doi.org/10.1016/j.seppur.2019.05.012

[6]   W.-K. Jo, J.-H. Park, H.-D. Chun, Photocatalytic destruction of VOCs for in-vehicle air cleaning, J. Photochem. Photobiol. A: Chem., 148 (2002) 109-119. https://doi.org/10.1016/S1010-6030(02)00080-1

[7]   A. Babuponnusami, K. Muthukumar, Advanced oxidation of phenol: a comparison between Fenton, electro-Fenton, sono-electro-Fenton and photo-electro-Fenton processes, Chem. Eng. J., 183 (2012) 1-9. https://doi.org/10.1016/j.cej.2011.12.010

[8]   H. Shemer, Y.K. Kunukcu, K.G. Linden, Degradation of the pharmaceutical metronidazole via UV, Fenton and photo-Fenton processes, Chemosphere, 63 (2006) 269-276. https://doi.org/10.1016/j.chemosphere.2005.07.029

[9]   K. Li, M.I. Stefan, J.C. Crittenden, Trichloroethene degradation by UV/H$_2$O$_2$ advanced oxidation process: product study and kinetic modeling, Environ, Sci. Technol., 41 (2007) 1696-1703. https://doi.org/10.1021/es0607638

[10]   K. Sivagami, R.R. Krishna, T. Swaminathan, Photo catalytic degradation of pesticides in immobilized bead photo reactor under solar irradiation, Solar Energ., 103 (2014) 488-493. https://doi.org/10.1016/j.solener.2014.02.001

[11]   N. Petit, A. Bouzaza, D. Wolbert, P. Petit, J. Dussaud, Photocatalytic degradation of gaseous perchloroethylene in continuous flow reactors: rate enhancement by chlorine radicals, Catalysis Today, 124 (2007) 266-272. https://doi.org/10.1016/j.cattod.2007.03.050

[12]   L.B.B. Ndong, M.P. Ibondou, X. Gu, M. Xu, S. Lu, Z. Qiu, Q. Sui, S.M. Mbadinga, Efficiently synthetic TiO$_2$ nano-sheets for PCE, TCE, and TCA degradations in aqueous phase under VUV irradiation, Water, Air, Soil Pollut., 225 (2014) 1951. https://doi.org/10.1007/s11270-014-1951-8

[13]   S. Yamazaki, T. Tanimura, A. Yoshida, K. Hori, Reaction mechanism of photocatalytic

degradation of chlorinated ethylenes on porous TiO2 pellets: Cl radical-initiated mechanism, J. Phys. Chem. A, 108 (2004) 5183-5188. https://doi.org/10.1021/jp0311310

[14] R.A. Monteiro, A.M. Silva, J.R. Ângelo, G.V. Silva, A.M. Mendes, R.A. Boaventura, V.J. Vilar, Photocatalytic oxidation of gaseous perchloroethylene over TiO_2 based paint, J. Photochem. Photobiol. A Chem., 311 (2015) 41-52. https://doi.org/10.1016/j.jphotochem.2015.06.007

[15] H. Yu, S. Lee, J. Yu, C. Ao, Photocatalytic activity of dispersed TiO2 particles deposited on glass fibers, J. Mol. Catal. A Chem., 246 (2006) 206-211. https://doi.org/10.1016/j.molcata.2005.11.007

[16] A. Basso, A.P. Battisti, R.d.F.P.M. Moreira, H.J. José, Photocatalytic effect of addition of TiO2 to acrylic-based paint for passive toluene degradation, Environ. Technol., (2018) 1-12. https://doi.org/10.1080/09593330.2018.1542034

[17] H. Rasoulnezhad, G. Hosseinzadeh, R. Hosseinzadeh, N. Ghasemian, Preparation of transparent nanostructured N-doped TiO_2 thin films by combination of sonochemical and CVD methods with visible light photocatalytic activity, J. Adv. Ceram., 7 (2018) 185-196. https://creativecommons.org/licenses/by/4.0/.

[18] S. Yamazaki, H. Tsukamoto, K. Araki, T. Tanimura, I. Tejedor-Tejedor, M.A. Anderson, Photocatalytic degradation of gaseous tetrachloroethylene on porous TiO_2 pellets, Appl. Catal. B Environ., 33 (2001) 109-117. https://doi.org/10.1016/S0926-3373(01)00167-9

[19] C. Martins, A.L. Cazetta, O. Pezoti, J.R. Souza, T. Zhang, E.J. Pilau, T. Asefa, V.C. Almeida, Sol-gel synthesis of new TiO_2/ activated carbon photocatalyst and its application for degradation of tetracycline, Ceram. Int., 43 (2017) 4411-4418. https://doi.org/10.1016/j.ceramint.2016.12.088

[20] Y. Liang, B. Zhou, N. Li, L. Liu, Z. Xu, F. Li, J. Li, W. Mai, X. Qian, N. Wu, Enhanced dye photocatalysis and recycling abilities of semi-wrapped TiO_2@ carbon nanofibers formed via foaming agent driving, Ceram. Int., 44 (2018) 1711-1718. https://doi.org/10.1016/j.ceramint.2017.10.101

[21] F.H. Abdulrazzak, Enhance photocatalytic activity of TiO_2 by carbon nanotubes, Int. J. Chem. Tech. Res., 9 (2016) 431-443. https://sphinxsai.com/chemtech.php

[22] H. Liang, Z. Jia, H. Zhang, X. Wang, J. Wang, Photocatalysis oxidation activity regulation of Ag/TiO2 composites evaluated by the selective oxidation of Rhodamine B, Appl. Surf. Sci., 422 (2017) 1-10. http://dx.doi.org/10.1016/j.apsusc.2017.05.211

[23] D. Zhang, J. Chen, P. Deng, X. Wang, Y. Li, T. Wen, Y. Li, Q. Xiang, Y. Liao, Hydrogen evolution promotion of Au-nanoparticles-decorated TiO_2 nanotube arrays prepared by dip-loading approach, J. Am. Ceram. Soc., 109 (2019) 5873-5880. https://doi.org/10.1111/jace.16441

[24] A. Martinez-Oviedo, S.K. Ray, H.P. Nguyen, S.W. Lee, Efficient photo-oxidation of NOx by Sn doped blue TiO2 nanoparticles, J. Photochem. Photobiol. A Chem., 370 (2019) 18-25. https://doi.org/10.1016/j.jphotochem.2018.10.032

[25] B. Niu, Z. Xu, From E-waste to Nb-Pb Co-doped and Pd-loaded TiO_2/ $BaTiO_3$ heterostructure: highly efficient photocatalytic performance, Chem. Sus. Chem., 12 (2019) 2819-2828. https://doi.org/10.1002/cssc.201900071.

[26] H. She, H. Zhou, L. Li, L. Wang, J. Huang, Q. Wang, Nickel-doped excess oxygen defect titanium dioxide for efficient selective photocatalytic oxidation of benzyl alcohol, ACS Sus. Chem. Eng., 6 (2018) 11939-11948. https://doi.org/10.1021/acssuschemeng.8b02217

[27] L. Zhang, W. Yu, C. Han, J. Guo, Q. Zhang, H. Xie, Q. Shao, Z. Sun, Z. Guo, Large scaled synthesis of heterostructured electrospun TiO2/SnO2 nanofibers with an enhanced

photocatalytic activity, J. Electrochem. Soc., 164 (2017) H651-H656. https://doi.org/10.1149/2.1531709jes

[28] F. Dong, S. Guo, H. Wang, X. Li, Z. Wu, Enhancement of the Visible Light Photocatalytic Activity of C-Doped TiO2 Nanomaterials Prepared by a Green Synthetic Approach, J. Phys. Chem. C, 115 (2011) 13285-13292. https://doi.org/10.1021/jp111916q

[29] G.B. Soares, B. Bravin, C.M. Vaz, C. Ribeiro, Facile synthesis of N-doped TiO2 nanoparticles by a modified polymeric precursor method and its photocatalytic properties, App. Catal. B Environ., 106 (2011) 287-294.https://doi.org/10.1016/j.apcatb.2011.05.018

[30] H. Li, D. Wang, H. Fan, P. Wang, T. Jiang, T. Xie, Synthesis of highly efficient C-doped TiO2 photocatalyst and its photo-generated charge-transfer properties, J. Colloid Interface Sci., 354 (2011) 175-180. https://doi.org/10.1016/j.jcis.2010.10.048

[31] T.-D. Pham, B.-K. Lee, Novel adsorption and photocatalytic oxidation for removal of gaseous toluene by V-doped TiO2/PU under visible light, J. Hazard. Mater., 300 (2015) 493-503. https://doi.org/10.1016/j.jhazmat.2015.07.048.

[32] J. Zhao, X. Yang, Photocatalytic oxidation for indoor air purification: a literature review, Build. Environ., 38 (2003) 645-654. https://doi.org/10.1016/S0360-1323(02)00212-3

[33] J. Mo, Y. Zhang, Q. Xu, J.J. Lamson, R. Zhao, Photocatalytic purification of volatile organic compounds in indoor air: A literature review, Atmos. Environ., 43 (2009) 2229-2246. https://doi.org/10.1016/j.atmosenv.2009.01.034

[34] M. Behpour, V. Atouf, Study of the photocatalytic activity of nanocrystalline S, N-codoped TiO2 thin films and powders under visible and sun light irradiation, Appl. Surf. Sci., 258 (2012) 6595-6601. https://doi.org/10.1016/j.apsusc.2012.03.085

[35] T. Sugimoto, X. Zhou, A. Muramatsu, Synthesis of uniform anatase TiO2 nanoparticles by gel–sol method: 3. Formation process and size control, J. Colloid Interface Sci., 259 (2003) 43-52. https://doi.org/10.1016/S0021-9797(03)00036-5

[36] G. Wu, T. Nishikawa, B. Ohtani, A. Chen, Synthesis and characterization of carbon-doped TiO2 nanostructures with enhanced visible light response, Chem. Mater., 19 (2007) 4530-4537. https://doi.org/10.1021/cm071244m

[37] S.Y. Treschev, P.-W. Chou, Y.-H. Tseng, J.-B. Wang, E.V. Perevedentseva, C.-L. Cheng, Photoactivities of the visible-light-activated mixed-phase carbon-containing titanium dioxide: The effect of carbon incorporation, Appl. Catal. B Environ., 79 (2008) 8-16. https://doi.org/10.1016/j.apcatb.2007.09.046

[38] J. Abisharani, S. Devikala, R.D. Kumar, M. Arthanareeswari, P. Kamaraj, Green synthesis of TiO2 Nanoparticles using Cucurbita pepo seeds extract, Mater. Today: Proc., 14 (2019) 302-307. https://doi.org/10.1016/j.matpr.2019.04.151

[39] A. Wanag, E. Kusiak-Nejman, J. Kapica-Kozar, A.W. Morawski, Photocatalytic performance of thermally prepared TiO2/C photocatalysts under artificial solar light, Micro & Nano Letters, 11 (2016) 202-206. https://doi.org/10.1049/mnl.2015.0507

[40] P. Zhang, C. Shao, Z. Zhang, M. Zhang, J. Mu, Z. Guo, Y. Liu, TiO2@ carbon core/shell nanofibers: controllable preparation and enhanced visible photocatalytic properties, Nanoscale, 3 (2011) 2943-2949. https://doi.org/10.1039/C1NR10269A

[SIP] SIP references (41-60s) have showed in supporting information page, http://journal.amecj.com/index.php/AMECJ-01